Original Article

JCBFM

Journal of Cerebral Blood Flow & Metabolism
2020, Vol. 40(9) 1849–1858

DOI: 10.1177/0271678X19874790
journals.sagepub.com/home/jcbfm
SAGE

Delayed clearance of cerebrospinal fluid tracer from choroid plexus in idiopathic normal pressure hydrocephalus

Per Kristian Eide[1,2], Lars Magnus Valnes[3], Are Hugo Pripp[4], Kent-Andre Mardal[3,5] and Geir Ringstad[2,6]

Abstract

Impaired clearance of amyloid-β from choroid plexus is one proposed mechanism behind amyloid deposition in Alzheimer's disease. The present study examined whether clearance from choroid plexus of a cerebrospinal fluid tracer, serving as a surrogate marker of a metabolic waste product, is altered in idiopathic normal pressure hydrocephalus (iNPH), one subtype of dementia. In a prospective observational study of close to healthy individuals (reference cohort; REF) and individuals with iNPH, we performed standardized T1-weighted magnetic resonance imaging scans before and through 24 h after intrathecal administration of a cerebrospinal fluid tracer (the magnetic resonance imaging contrast agent gadobutrol). Changes in normalized T1 signal within the choroid plexus and cerebrospinal fluid of lateral ventricles were quantified using FreeSurfer. The normalized T1 signal increased to maximum within choroid plexus and cerebrospinal fluid of lateral ventricles 6–9 h after intrathecal gadobutrol in both the REF and iNPH cohorts (enrichment phase). Peak difference in normalized T1 signals between REF and iNPH individuals occurred after 24 h (clearance phase). The results gave evidence for gadobutrol resorption from cerebrospinal fluid by choroid plexus, but with delay in iNPH patients. Whether choroid plexus has a role in iNPH pathogenesis in terms of delayed clearance of amyloid-β remains to be shown.

Keywords

Idiopathic normal pressure hydrocephalus, choroid plexus, cerebrospinal fluid, CSF tracer, clearance, magnetic resonance imaging, intrathecal contrast agents, glymphatic, humans

Received 21 December 2018; Revised 29 June 2019; Accepted 1 July 2019

Introduction

The choroid plexus is a highly vascularized tissue located in the cerebral ventricles and has traditionally been considered a main source of cerebrospinal fluid (CSF) production, thereby being a driving force behind CSF bulk flow from the ventricular system to the subarachnoid space.[1–3] More recently, the choroid plexus has emerged as a vital structure for neuroprotection, neuro-immune regulation, and homeostasis of the brain's chemical milieu in a broad sense.[4] Experimental research also provides evidence that the choroid plexus has a function in clearance of amyloid-β from the CSF, thus playing a role in the pathogenesis of Alzheimer's disease.[5,6]

The description of the cerebral glymphatic system in 2012[7] and the demonstration of dural lymphatic vessels in 2015[8,9] have facilitated renewed interest in the mechanisms behind clearance of metabolic waste solutes from the brain. Impaired glymphatic[7] and lymphatic[10] function may both lead to impaired clearance of metabolic waste products, such as amyloid-β, which in

[1]Department of Neurosurgery, Oslo University Hospital – Rikshospitalet, Oslo, Norway
[2]Faculty of Medicine, Institute of Clinical Medicine, University of Oslo, Oslo, Norway
[3]Department of Mathematics, University of Oslo, Oslo, Norway
[4]Oslo Centre of Biostatistics and Epidemiology, Research Support Services, Oslo University Hospital, Oslo, Norway
[5]Center for Biomedical Computing, Simula Research Laboratory, Lysaker, Norway
[6]Division of Radiology and Nuclear Medicine, Department of Radiology, Oslo University Hospital – Rikshospitalet, Oslo, Norway

Corresponding author:
Per Kristian Eide, Department of Neurosurgery, Oslo University Hospital – Rikshospitalet, PB 4950 Nydalen, Oslo 0424, Norway.
Email: peide@ous-hf.no

neuro-degenerative disease may accumulate and cause toxic damage to the brain. We previously demonstrated impaired glymphatic clearance of a magnetic resonance imaging (MRI) contrast agent (gadobutrol), serving as a CSF tracer in individuals with idiopathic normal pressure hydrocephalus (iNPH).[11–13] This CSF tracer is a molecule of size 604 Da that may serve as a surrogate marker of clearance of metabolic waste products from brain. The disease iNPH is characterized by dementia, gait ataxia, urinary incontinence and enlarged size of the cerebral ventricles,[14] and is characterized by neuro-degeneration and deposition of amyloid-β in a significant proportion of the patients.[15] Another feature of this entity is the significant alterations of the CSF circulation. Therefore, CSF diversion surgery may provide sustained clinical improvement even though with some reduction of treatment effect over time.[16]

Given the important role of impaired cerebral clearance function for evolvement of neuro-degeneration and dementia, characterizing the underlying mechanisms seems crucial. While glymphatic clearance seems reduced in iNPH patients,[11–13] it remains unknown whether or not clearance from the choroid plexus is reduced. In this present study, we for the first time utilized a CSF tracer for in vivo assessment of choroid plexus clearance function in references and a cohort with a dementia disease.

Materials and methods

Patients and study design

The study was approved by the Regional Committee for Medical and Health Research Ethics (REK) of Health Region South-East, Norway (2015/96), the Institutional Review Board of Oslo university hospital (2015/1868), and the National Medicines Agency (15/04932-7). The conduct of the study was governed by ethical standards according to the Helsinki Declaration of 1975 (and as revised in 1983). Study participants were included after written and oral informed consent.

A prospective and observational study design was used, and included consecutive patients with suspected CSF leakage, causative of idiopathic intracranial hypotension, and patients with iNPH. All individuals underwent MRI before and at several time points following intrathecal lumbar injection of the MRI contrast agent gadobutrol during a study period from October 2015 to September 2016.

Exclusion criteria were: History of hypersensitivity reactions to contrast agents, history of severe allergy reactions in general, evidence of renal dysfunction, pregnant or breastfeeding women, and age <18 or >80 years.

The reference (REF) subjects had a tentative diagnosis of idiopathic intracranial hypotension and were referred to the Department of Neurosurgery, Oslo University Hospital – Rikshospitalet, Oslo, Norway, from local neurological departments for clinical work-up of suspected CSF leakage. They underwent MRI with intrathecal gadobutrol with the primary indication to define site of CSF leakage, and were recruited prospectively and consecutively in parallel with iNPH patients. Patients with iNPH were referred to the Department of Neurosurgery, Oslo University Hospital – Rikshospitalet, Oslo, Norway, from local neurological departments, based on clinical symptoms and findings indicative of iNPH, and imaging findings of ventriculomegaly. Within the Department of Neurosurgery, clinical severity was graded based on a previously described NPH grading scale.[16,17] Patients were selected for shunt surgery based on assessing clinical symptoms and findings, imaging findings, co-morbidity, and results of intracranial pressure (ICP) monitoring, as previously described.[16,17]

MRI protocol

A 3 Tesla Philips Ingenia MRI scanner (Philips Medical systems, Best, The Netherlands) with equal imaging protocol settings at all the time points was applied to acquire sagittal 3D T1-weighted volume scans with ultrafast gradient echo and preparation pulse (T1 FFE). The following imaging parameters were used: repetition time (TR) = "shortest" (typically 5.1 ms), echo time (TE) = "shortest" (typically 2.3 ms), inversion time = 853 ms, flip angle (FA) = 8 degrees, field of view (FOV) = 256 × 256 mm, and matrix = 256 × 256 pixels (reconstructed 512 × 512). We sampled 184 over-contiguous (overlapping) slices with 1 mm thickness, which was automatically reconstructed to 368 slices with 0.5 mm thickness.

In addition, a T2-weighted volume acquisition (T2 VISTA) was obtained with the following parameters: TR = 2500 ms, TE = 330 ms, FA = 90 degrees, FOV = 250 × 250 mm, matrix size = 252 × 250 pixels.

Intrathecal administration of gadobutrol

After the pre-contrast MRI exam, an interventional neuroradiologist performed X-ray-guided lumbar puncture. Correct position of the syringe tip in the subarachnoid space was verified by CSF backflow from the puncture needle, and a small amount (typically 3 ml) of 270 mg I/ml iodixanol (Visipaque™, GE Healthcare, USA) was injected to confirm unrestricted distribution of radiopaque contrast agent in the lumbar SAS. Then, 0.5 ml of 1.0 mmol/ml gadobutrol (Gadovist™, Bayer Pharma AG, Berlin, Germany) was injected

intrathecally through the same needle. Following removal of the needle, the study subjects were instructed to rotate themselves around the long axis of the body once before transportation back to the MRI suite, while remaining in the supine position.

Post-contrast MRI acquisitions

Consecutive, identical MRI acquisitions using the previously outlined MRI protocol parameters were performed after intrathecal gadobutrol administration. The study participants were instructed to remain supine in bed. One pillow under the head allowed for up to 15 degrees head elevation, and all transfer of study subjects between the neurosurgical department and the MRI suite, and between the bed and the MRI table, was performed by the hospital staff to help the patient remain in the supine position. Patients and controls were allowed to move without any restrictions between the 4 p.m. examination at the end of day one and the 24 h scan next morning.

While the MRI exams, for practical reasons, could not be obtained at identical time points for every study subject, all exams were categorized into the following time intervals: Pre-contrast, 1.5–2 h, 2–4 h, 4–6 h, 6–9 h, 24 h and 48 h.

Image analysis

The FreeSurfer software (version 6.0) (http://surfer.nmr.mgh.harvard.edu/) was used for segmentation, parcellation, and registration/alignment of the longitudinal data. The segmentation and parcellation acquired from FreeSurfer were used to investigate the increase of T1 signal intensity due to CSF tracer enhancement. The methods are documented in a review.[18] In this study, we segmented the choroid plexus within the lateral ventricles as well as the CSF within the lateral ventricles.

The MR images of each patient were used to create a median template registered to the baseline, the process of which has been previously described.[19] Hence, for each patient, the MR images were registered to the corresponding template using a rigid transformation.[19] The registrations were subsequently checked manually by one of the co-authors (LMV), and no significant errors were visible.

The T2-weighted images (except for three iNPH patients who had no T2 images) were also used for the segmentation with FreeSurfer. Additionally, the specification of large ventricles was added to the segmentation processes for the iNPH patients.

The segmentation of seven iNPH patients was edited due to segmentation errors. The corrections were automatic based on the patients T2 image, except in one iNPH patient who had no T2 image, which required manual editing to correct. Notably, the segmentation procedure did not impact the measured T1 signal units within the regions of interest (Supplementary Figure 1).

We determined the volume of choroid plexus and lateral ventricles, which was done by summarizing all voxels with the same segmentation. The corrections of the lateral ventricle volumes were done by labeling voxels in the near vicinity of the lateral ventricles, such as white matter and choroid plexus.

T1 signal derived parameters

For each segmented area, the median T1 signal unit was computed for each time point. Further, the median signal unit was divided against the signal unit of a reference ROI placed within the posterior part of the superior sagittal sinus in axially reconstructed images from the same T1 volume scan. The ratio refers to as *normalized T1 signal units* and corrects for any baseline changes of image grey scale due to potential image scaling between single scans. Previous observations indicate no measureable enhancement of contrast agent at MRI in the reference location after intrathecal injection of gadobutrol at this concentration.[11]

Estimation of CSF tracer concentration in lateral ventricle

The CSF tracer concentration (C) causes the T1 time to be shortened with the following relation

$$1/\mathrm{T1} = 1/\mathrm{T1}(0) + \mathrm{R} \times \mathrm{C} \quad (1)$$

According to Lu et al.,[20] we assumed that $\mathrm{T1}(0) = 4300\,\mathrm{ms}$, and with reference to Rohrer et al.,[21] the relaxivity constant $\mathrm{R} = 3.2\,\mathrm{mM}^{-1}\mathrm{s}^{-1}$. Since imaging parameters are the same for each T1 image, the T1-time becomes the only variable in the T1 protocol signal equation (equation (1)) in Gowland et al.[22] Then the concentration C is estimated by computing the normalized T1 signal increase from baseline that is needed to achieve the average signal increase.

Statistical analysis

A linear mixed model for repeated measurements with a random intercept for study participant using maximum likelihood estimation with robust standard errors analyzed the effect of segment (i.e. choroid plexus versus CSF) and cohort (i.e. REF versus iNPH) on normalized T1 signal units at the time interval from 4 to 24 h. In addition to the main fixed effects of segment, cohort and age, the statistical model included an interaction term between segment and cohort. The interaction term assessed the modifying effect of cohort on normalized

T1 signal units in segment. Thus, a statistical significant interaction term could indicate that the mean difference in normalized T1 signal units between choroid plexus and CSF was different in the iNPH and REF cohort.

Statistical significance was accepted at the 0.05 level. The descriptive statistics was performed using the SPSS software version 20 (IBM Corporation, Armonk, NY), and the linear mixed model analysis was performed with Stata/SE 15.0 for Windows (Stata Corp LLC, College Station, TX).

Results

The study included two cohorts of eight REF and nine iNPH patients, respectively (Table 1). The REF individuals had a tentative diagnosis of idiopathic intracranial hypotension due to CSF leakage, which was confirmed in 3/8 individuals. No CSF leakage was seen in 5/8 individuals, who we consider close to healthy. However, the patient cohorts differed in several respects (Table 1).

Table 2 presents measures of ventriculomegaly/CSF circulation failure (Evans index, callosal angle, and disproportionately enlarged subarachnoid space hydrocephalus, DESH), as well as volume of choroid plexus in lateral ventricle and lateral ventricular volume size in REF and iNPH individuals. We found no differences in volume of choroid plexus between patient cohorts, while volumes of CSF spaces were larger in the iNPH cohort (Table 2).

After intrathecal administration of the CSF tracer (i.e. MRI contrast agent), tracer propagated into the ventricular system and enriched the choroid plexus of both REF and iNPH individuals (Figure 1). This was, however, markedly more pronounced in iNPH than REF subjects. The changes in signal unit ratios within choroid plexus of lateral ventricles and the CSF of lateral ventricles of the (a) REF and (b) iNPH cohorts are illustrated in Figure 2. For both locations, the tracer enrichment was more pronounced in the iNPH than in REF individuals (Figure 2). Moreover, Table 3 presents the percentage change in normalized T1 signal from before CSF tracer administration within choroid plexus and lateral ventricle of the REF and iNPH cohorts. While tracer enrichment within the lateral ventricle of REF individuals was close to significant ($P = 0.052$), the MRI signal increased significantly ($P < 0.001$) at the other locations (Table 3).

While a CSF leakage was verified in 3/8 REF patients, the presence of CSF leakage seemed not to impact the measured T1 signal units. We found no differences in normalized T1 signal units between those individuals with/without verified leakage at any time

Table 2. Radiological measures and volumes of cerebral ventricles and choroid plexus of REF and iNPH cohorts.

	REF	iNPH	Significance
Evans index	0.30 ± 0.05	0.38 ± 0.04	0.001
DESH (Y/N)	0/8	6/3	ns
Callosal angle (degrees)	117.3 ± 14.3	76.3 ± 29.0	0.003
Volume measures (ml)			
Choroid plexus	0.75 ± 0.22	0.88 ± 0.23	ns
CSF, lateral ventricle	14.83 ± 14.43	68.85 ± 18.52	<0.001

Note: Categorical data presented as numbers; continuous data presented as mean ± standard deviation. Significant differences between groups were determined by Pearson Chi-square test for categorical data and by independent samples t-test for continuous data. CSF: cerebrospinal fluid; DESH: disproportionate enlargement of subarachnoid spaces hydrocephalus; iNPH: idiopathic normal pressure hydrocephalus; REF: reference patients.

Table 1. Demographic and clinical information about the REF and iNPH cohorts at the time MRI.

	REF	iNPH	Significance
N	8	9	
Sex (F/M)	6/2	1/8	0.008
Age (years)	38.4 ± 17.3	68.3 ± 9.5	<0.001
Symptoms reported by patient and/or family			
Gait disturbance	2 (25%)	9 (100%)	0.001
Urinary incontinence	0 (0%)	6 (67%)	0.004
Cognitive impairment	0 (0%)	8 (89%)	<0.001
Duration of symptoms (months)	42.4 ± 40.6	21.3 ± 10.4	ns
NPH score	15 (14–15)	13 (11–13)	<0.001

Note: Categorical data presented as numbers; continuous data presented as mean ± standard deviation. Significant differences between groups were determined by Pearson Chi-square test for categorical data and by independent samples t-test for continuous data. iNPH: idiopathic normal pressure hydrocephalus; REF: reference patients.

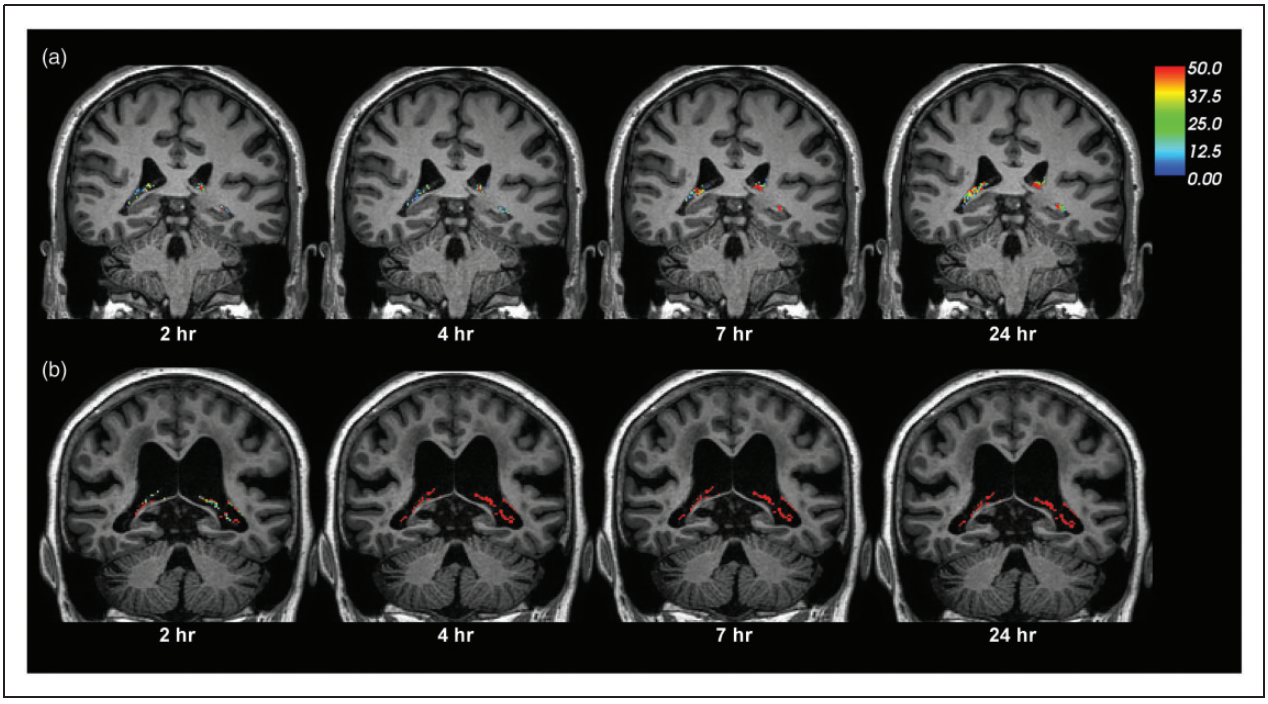

Figure 1. CSF tracer enrichment over time within the choroid plexus of a REF and an iNPH subject. The enrichment of CSF tracer within choroid plexus over time is shown for (a) a REF and (b) an iNPH subject. The percentage change in signal unit ratio is indicated at the color scale. Signal change within the CSF spaces is extracted in order to only present the percentage signal change within the choroid plexus.

point, neither the choroid plexus (lowest P-value 0.34) nor the CSF of the lateral ventricle (lowest P-value 0.21) (data not shown).

Figure 2 indicates that both choroid plexus enhancement and clearance of CSF tracer was different from REFs in the iNPH patients. Significant differences were seen during the enhancement phase after 4–6 and 6–9 h, as well as during the clearance phase at 24 h (Table 3). In particular, the most pronounced difference between REF and iNPH in choroid plexus was seen after 24 h, indicative of delayed clearance of CSF tracer from choroid plexus in iNPH disease.

Estimation of CSF tracer concentration and level also gave evidence for delayed clearance from lateral ventricle in iNPH. Table 4 presents the concentration and level of CSF tracer in lateral ventricle of iNPH and REF individuals, estimated according to equation (1). Concentrations for REF individuals were 0.0079 and 0.0022 mM after 6–9 and 24 h, respectively, while corresponding numbers in iNPH were 0.031 and 0.024 mM. As such, the reduction of tracer in lateral ventricles during this period in iNPH and REF was 23% and 72%, respectively, in a relative sense. On the other hand, in iNPH, the combination of increased volume of lateral ventricles and more pronounced CSF tracer enrichment resulted in increased absolute amounts of CSF tracer of 2.13 and 1.65 μmol after 6–9 and 24 h, respectively. In an absolute sense, the corresponding reduction in CSF tracer levels from 6–9 to 24 h after tracer administration was −0.48 and −0.0057 μmol, respectively.

To further test whether the clearance of CSF tracer from choroid plexus per se was significantly different in iNPH, we determined the interaction term whether the iNPH diagnosis itself modified the CSF tracer enrichment within the choroid plexus and CSF of lateral ventricle. As indicated in Figure 3, a significant interaction term provided evidence for delayed clearance of CSF tracer from choroid plexus of iNPH compared to REF. Hence, in iNPH, enhancement was higher in CSF compared to choroid plexus, while in REF subjects, enhancement was higher in choroid plexus compared to CSF (Figure 3). Moreover, after correcting the interaction presented in Figure 3 for age-differences between REF and iNPH cohorts, the interaction term between REF and iNPH individuals remained significant. That is, the differences in CSF tracer enhancement within choroid plexus could not be explained by age-differences between REF and iNPH subjects.

Discussion

The present data indicate that the MRI contrast agent gadobutrol is resorbed from CSF by the choroid plexus

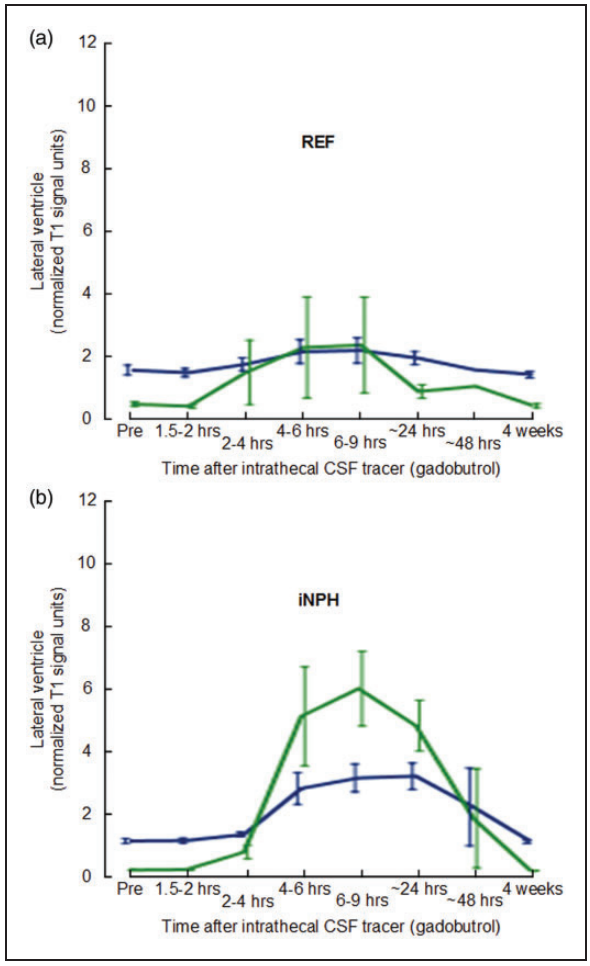

Figure 2. CSF tracer enrichment in choroid plexus and CSF of lateral ventricle in the REF and iNPH cohorts. Trend plots of signal unit ratios are shown for choroid plexus (blue lines) and CSF (green lines) within lateral ventricle of (a) REF and (b) iNPH subjects. The trend plots are shown as mean ± standard error (SE). iNPH: idiopathic normal pressure hydrocephalus; REF: reference patients.

of the lateral ventricles. In iNPH patients, CSF enrichment of gadobutrol exceeded that of choroid plexus and was opposite to observations made in a cohort of healthy, or close to healthy, subjects. The findings suggest delayed clearance of molecules with similar features from choroid plexus in iNPH.

Patients

The iNPH cohort was older than the reference cohort. An effect of age on results of CSF tracer clearance could therefore be anticipated. However, the differences in CSF tracer enrichment within choroid plexus and CSF of REF and iNPH individuals remained consistent after adjusting for age in the statistical analysis.

Table 3. Percentage change in signal unit ratios at various time points after intrathecal gadobutrol in REF and iNPH patients.

		Time after i.th. gadobutrol													
Anatomical region		Enhancement phase						Clearance phase						Overall significance	
[FreeSurfer]	Group	1.5–2 h	P	2–4 h	P	4–6 h	P	6–9 h	P	24 h	P	48 h	4 weeks	P	
Choroid plexus [31, 63]	REF	−3 ± 8	ns	22 ± 65	ns	57 ± 107	0.055	56 ± 118	0.019	24 ± 34	0.004	39	−8 ± 15	ns	<0.001
	iNPH	7 ± 25		21 ± 26		162 ± 127		191 ± 121		185 ± 112		108 ± 141	0 ± 18		<0.001
CSF, lateral ventricle [4, 43]	REF	−10 ± 8	ns	342 ± 957	ns	641 ± 1415	0.023	656 ± 1438	0.002	173 ± 325	0.001	228	−10 ± 12	ns	0.052
	iNPH	11 ± 28		296 ± 350		2598 ± 2179		3041 ± 1808		2272 ± 1217		869 ± 1104	−7 ± 19		<0.001

Note: Continuous variables given as mean ± standard deviation. P: Statistically significant differences determined by a linear mixed model for repeated measurements with time interval as fixed effect and a random intercept for patient. Numbers in brackets refer to FreeSurfer regions. iNPH: idiopathic normal pressure hydrocephalus; REF: reference patients.

Table 4. Estimated concentration of CSF tracer within lateral ventricles of REF and iNPH patients.

	REF		iNPH	
Volume CSF, lateral ventricles (ml)	14.287		68.845	
Time after i.th. CSF tracer	6–9 h	24 h	6–9 h	24 h
Signal increase from baseline (ratio)	7.56	2.73	31.41	23.72
Concentration, CSF tracer (mM)	0.0079	0.0022	0.031	0.024
Change in concentration of CSF tracer from 6–9 h to 24 h (mM)	−0.0057		−0.007	
Level of CSF tracer (μmol)	0.11	0.033	2.13	1.65
Change in level of CSF tracer from 6–9 h to 24 h (μmol)	−0.077		−0.48	

Note: The concentrations and levels of CSF tracer within the lateral ventricles were computed according to equation (1), see Materials and Methods section. CSF: cerebrospinal fluid; iNPH: idiopathic normal pressure hydrocephalus; REF: reference patients.

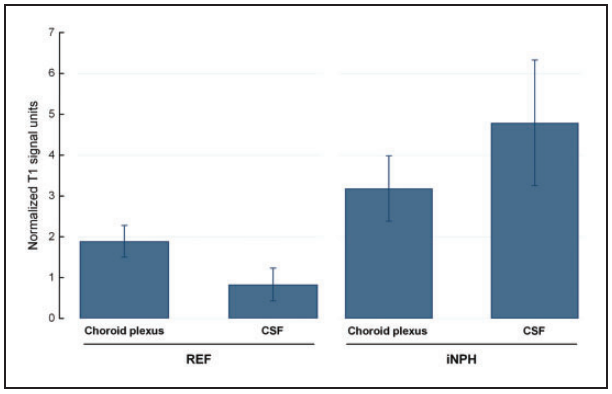

Figure 3. Analysis of interaction between signal unit ratio within CSF of lateral ventricle and choroid plexus in REF and iNPH cohorts at 24 h. The mean relative signal unit ratios within choroid plexus and CSF of the lateral ventricle are shown for the REF and iNPH subjects. Hence, the mean difference in normalized T1 signal unit between choroid plexus and CSF was different in the iNPH than REF subjects (interaction term, $P < 0.001$), and the mean normalized T1 signal in choroid plexus was higher in the iNPH than REF subjects ($P = 0.004$). The observation suggests impaired clearance of CSF tracer from choroid plexus of iNPH than REF individuals. Error bars are 95% CI.
iNPH: idiopathic normal pressure hydrocephalus; CSF: cerebrospinal fluid; REF: reference patients.

Clearance of molecules from lateral ventricles

In the present study, the combined increased lateral ventricular volume and increased CSF tracer enrichment gave 19.4 and 50.0 times higher CSF tracer amounts in the lateral ventricles of iNPH patients, as compared with REF individuals after 6–9 and 24 h, respectively. The increased CSF tracer enhancement in lateral ventricles is related to CSF flow alterations in iNPH. We are currently investigating whether the retrograde aqueductal flow of CSF in iNPH patients, as previously reported by us,[11,23] explains the increase.

The present results extended previous data showing that during clearance phase (from 6–9 h to 24 h after CSF tracer administration), the relative reduction of CSF tracer concentration in lateral ventricles of iNPH was one third that of REF, but was much larger in absolute terms. Accordingly, while the relative reduction of CSF tracer was reduced in iNPH compared to REF individuals, the reduction of CSF tracer in absolute terms was higher in iNPH, due to the stronger enrichment of ventricular CSF tracer in this latter patient group. First, we assume that clearance of CSF tracer is both trans-ependymal and via choroid plexus. The trans-ependymal route is indicated by strong periventricular tracer enrichment in iNPH.[11,12] Second, since the CSF tracer is biologically inert, it may seem less likely that the choroid plexus has an active role in removing CSF tracer; rather, the relative reduction is by passive clearance of tracer.

Clearance of molecules from choroid plexus

Several studies have demonstrated that reduced function of choroid plexus may be involved in disease processes causing neurodegeneration and Alzheimer's disease.[4,6,24,25] The present results provide in vivo evidence of reduced clearance of a molecule from choroid plexus of iNPH individuals. While tracer supply in CSF was higher in iNPH due to ventricular reflux, tracer enhancement in plexus was proportionally lower than in REF (Figure 3). In line with this assumption, experimental studies have shown reduced clearance of amyloid-β from choroid plexus, suggesting a role in the pathogenesis of Alzheimer's disease.[5,6] We consider the CSF tracer used in this study as a surrogate marker of cerebral waste products in general, but how well the present CSF tracer depicts the behavior of soluble amyloid-β has not been determined. It has already been established that the choroid plexus has a role in absorption of a range of other macromolecules from

CSF, for example, drugs such as penicillin and other endogenous and exogenous solutes.[2]

While this study provides evidence for transfer of an MRI contrast agent over the CSF–blood–barrier, transport of MRI contrast agents in the other direction, i.e. from blood to CSF, has recently been seen in several studies.[26–28] In rats, the concentration of MRI contrast agent in CSF was clearly higher than in blood after 4.5 h, and most likely leaked into ventricular CSF through the choroid plexus.[28] It may not seem reasonable that the highly vascularized choroid plexus should be a site for one-way traffic of substances from blood to CSF. Others have previously provided evidence of bidirectional exchange of substances from the choroid plexus,[29–31] i.e. both from the blood and into the CSF and from the CSF into the blood.

Absorption of CSF by the choroid plexus was first suggested almost one hundred years ago by Foley in 1921 (reviewed by McComb[32]) and later in hydrocephalic infants,[31] but has been contradicted by others.[33] A recent review[34] concluded that further investigation is required to establish the role of the choroid plexus in absorption of CSF.

Role of choroid plexus in CSF production

It has traditionally been considered that the choroid plexus is the main source of CSF production,[35–37] while minor contributions to CSF production have been attributed to extra-ventricular sources such as the brain ependyma and parenchyma,[32,38] and spinal cord ependyma.[39] However, the traditional view of choroid plexus being the main producer of CSF has been heavily criticized.[3,36,40] It is now clear that the subarachnoid CSF compartment is continuous with the entire paravascular compartment of the brain and spinal cord not only in animals[7,41–43] but also in humans.[12] New insights of continuous bi-directional fluid exchange over the entire blood–brain barrier clearly render for extra-choroidal CSF production.[36]

The present observations of significantly increased enhancement and delayed clearance of CSF tracer might also be attributed to reduced CSF tracer washout due to reduced CSF production in choroid plexus of iNPH. Experimental data from ageing rats and humans with iNPH or Alzheimer's disease have shown reduced production of CSF from choroid plexus and impaired turnover of CSF.[44] After intrathecal administration of an MRI contrast agent as CSF tracer, clearance of the CSF tracer from CSF spaces was significantly reduced, indicative of reduced CSF turnover in iNPH.[11–13] The reduced CSF turnover within CSF spaces in iNPH was accompanied with delayed brain-wide clearance of CSF tracers that were interpreted as impaired glymphatic clearance,[11,12] and suggested a common pathway behind iNPH and Alzheimer's dementia and explains why amyloid-β deposits in brain tissue overlap significantly in these conditions.[45]

Others have reported that the function of choroid plexus changes during ageing and in CSF circulation failure.[40] The iNPH cohort in this study was significantly older than the REF group. Furthermore, reduced CSF production in iNPH might be associated with increased pulsatile ICP and to lesser extent, increased static ICP, which is characteristic of iNPH patients responding to CSF diversion surgery.[17] Several authors have previously reported that CSF production can be reduced as response to an increased ICP caused by hydrocephalus.[46–48]

A link between CSF production and glymphatic function is to be expected. Probably, a certain magnitude of CSF production is required to maintain sufficient CSF pressure to drive paravascular clearance pathways throughout the brain[7,49,50] and to drive lymphatic efflux of waste molecules from the craniospinal compartment.[51] This view is in contrast to the previous concept that CSF production is primarily required for mechanical protection of the brain and maintenance of the electrolytic environment and acid–base balance.[52]

Limitations

It should be noted that different levels of CSF tracer enhancement do not directly reflect changes in the concentration levels of the CSF tracer. The present results do therefore not provide measures by absolute quantities, even though such quantities may be estimated according to equation (1). T1 maps might be used for absolute quantifications of CSF tracer in future studies.

While the choroid plexus is present in all cerebral ventricles, this study only examined choroid plexus in lateral ventricles. We would, however, expect results to be similar for all compartments.

Conclusions

The present study indicates that the MRI contrast agent gadobutrol is absorbed by the choroid plexus when utilized as CSF tracer. In patients with iNPH, this CSF tracer enhanced more strongly and was cleared with slower rate, from choroid plexus as compared to in REF subjects. Delayed CSF clearance of brain metabolites through choroid plexus may be instrumental for neurodegeneration in iNPH dementia.

Funding

The author(s) received no financial support for the research, authorship, and/or publication of this article.

Acknowledgements

We thank Dr. Øivind Gjertsen, Dr. Bård Nedregaard and Dr. Ruth Sletteberg from the Department of Radiology, Oslo University Hospital – Rikshospitalet, who performed the intrathecal gadobutrol injections in all study subjects. We also sincerely thank the Intervention Centre and Department of Neurosurgery at the Oslo University Hospital – Rikshospitalet for providing valuable support with MR scanning and care-taking of all study subjects throughout the study. Finally, we sincerely thank the Nurse Staff and Hydrocephalus outward clinic, Department of Neurosurgery, Oslo University Hospital – Rikshospitalet for care-taking of all study subjects throughout the study.

Declaration of conflicting interests

The author(s) declared no potential conflicts of interest with respect to the research, authorship, and/or publication of this article.

Authors' contributions

Conceptualization and design: PKE, LMV, KAM, GR. Investigation, formal analysis and visualization: PKE, LMV, KAM, GR. Supervision, Administration and writing – original draft: PKE, GR. Statistical analysis: AHP. Writing, review and editing: PKE, LMV, AHP, KAM, GR. All authors (PKE, LMV, AHP, KAM, GR) approved the final version of the article. Correspondence and material requests: PKE.

ORCID iD

Per Kristian Eide https://orcid.org/0000-0001-6881-9280

Supplemental material

Supplemental material for this paper can be found at the journal website: http://journals.sagepub.com/home/jcb

References

1. Praetorius J. Water and solute secretion by the choroid plexus. *Pflugers Arch* 2007; 454: 1–18.
2. Spector R, Keep RF, Robert Snodgrass S, et al. A balanced view of choroid plexus structure and function: focus on adult humans. *Exp Neurol* 2015; 267: 78–86.
3. Oreskovic D, Rados M and Klarica M. Role of choroid plexus in cerebrospinal fluid hydrodynamics. *Neuroscience* 2017; 354: 69–87.
4. Ghersi-Egea JF, Strazielle N, Catala M, et al. Molecular anatomy and functions of the choroidal blood-cerebrospinal fluid barrier in health and disease. *Acta Neuropathol* 2018; 135: 337–361.
5. Crossgrove JS, Li GJ and Zheng W. The choroid plexus removes beta-amyloid from brain cerebrospinal fluid. *Exp Biol Med* 2005; 230: 771–776.
6. Serot JM, Zmudka J and Jouanny P. A possible role for CSF turnover and choroid plexus in the pathogenesis of late onset Alzheimer's disease. *J Alzheimer's Dis* 2012; 30: 17–26.
7. Iliff JJ, Wang M, Liao Y, et al. A paravascular pathway facilitates CSF flow through the brain parenchyma and the clearance of interstitial solutes, including amyloid beta. *Sci Transl Med* 2012; 4: 147ra111.
8. Louveau A, Smirnov I, Keyes TJ, et al. Structural and functional features of central nervous system lymphatic vessels. *Nature* 2015; 523: 337–341.
9. Aspelund A, Antila S, Proulx ST, et al. A dural lymphatic vascular system that drains brain interstitial fluid and macromolecules. *J Exp Med* 2015; 212: 991–999.
10. Da Mesquita S, Louveau A, Vaccari A, et al. Functional aspects of meningeal lymphatics in ageing and Alzheimer's disease. *Nature* 2018; 560: 185–191.
11. Ringstad G, Vatnehol SAS and Eide PK. Glymphatic MRI in idiopathic normal pressure hydrocephalus. *Brain* 2017; 140: 2691–2705.
12. Ringstad G, Valnes LM, Dale AM, et al. Brain-wide glymphatic enhancement and clearance in humans assessed with MRI. *JCI Insight* 2018; 3: 1–16.
13. Eide PK and Ringstad G. Delayed clearance of cerebrospinal fluid tracer from entorhinal cortex in idiopathic normal pressure hydrocephalus: a glymphatic magnetic resonance imaging study. *J Cereb Blood Flow Metab* 2019; 39: 1355–1368.
14. Malm J and Eklund A. Idiopathic normal pressure hydrocephalus. *Pract Neurol* 2006; 6: 14–27.
15. Leinonen V, Koivisto AM, Savolainen S, et al. Amyloid and TAU proteins in cortical brain biopsy and Alzheimer's disease. *Ann Neurol* 2010; 68: 446–453.
16. Eide PK and Sorteberg W. Outcome of surgery for idiopathic normal pressure hydrocephalus: role of preoperative static and pulsatile intracranial pressure. *World Neurosurg* 2016; 86: 186–193.e181.
17. Eide PK and Sorteberg W. Diagnostic intracranial pressure monitoring and surgical management in idiopathic normal pressure hydrocephalus: a 6-year review of 214 patients. *Neurosurgery* 2010; 66: 80–91.
18. Fischl B. FreeSurfer. *Neuroimage* 2012; 62: 774–781.
19. Reuter M, Schmansky NJ, Rosas HD, et al. Within-subject template estimation for unbiased longitudinal image analysis. *Neuroimage* 2012; 61: 1402–1418.
20. Lu H, Nagae-Poetscher LM, Golay X, et al. Routine clinical brain MRI sequences for use at 3.0 Tesla. *J Magn Reson Imaging* 2005; 22: 13–22.
21. Rohrer M, Bauer H, Mintorovitch J, et al. Comparison of magnetic properties of MRI contrast media solutions at different magnetic field strengths. *Invest Radiol* 2005; 40: 715–724.
22. Gowland PA and Leach MO. Fast and accurate measurements of T1 using a multi-readout single inversion-recovery sequence. *Magn Reson Med* 1992; 26: 79–88.
23. Lindstrom EK, Ringstad G, Mardal KA, et al. Cerebrospinal fluid volumetric net flow rate and direction in idiopathic normal pressure hydrocephalus. *NeuroImage Clin* 2018; 20: 731–741.
24. Gonzalez-Marrero I, Gimenez-Llort L, Johanson CE, et al. Choroid plexus dysfunction impairs beta-amyloid clearance in a triple transgenic mouse model of Alzheimer's disease. *Front Cell Neurosci* 2015; 9: 17.

25. Krzyzanowska A and Carro E. Pathological alteration in the choroid plexus of Alzheimer's disease: implication for new therapy approaches. *Front Pharmacol* 2012; 3: 75.
26. Berger F, Kubik-Huch RA, Niemann T, et al. Gadolinium distribution in cerebrospinal fluid after administration of a gadolinium-based MR contrast agent in humans. *Radiology* 2018; 288: 703–709.
27. Nehra AK, McDonald RJ, Bluhm AM, et al. Accumulation of gadolinium in human cerebrospinal fluid after gadobutrol-enhanced MR imaging: a prospective observational cohort study. *Radiology* 2018; 288: 416–423.
28. Jost G, Frenzel T, Lohrke J, et al. Penetration and distribution of gadolinium-based contrast agents into the cerebrospinal fluid in healthy rats: a potential pathway of entry into the brain tissue. *Eur Radiol* 2017; 27: 2877–2885.
29. Dichiro G. Movement of the cerebrospinal fluid in human beings. *Nature* 1964; 204: 290–291.
30. Hassin GB. Notes on the nature and origin of the cerebrospinal fluid. *J Nerv Ment Dis* 1924; 59: 113–121.
31. Milhorat TH, Mosher MB, Hammock MK, et al. Evidence for choroid-plexus absorption in hydrocephalus. *N Engl J Med* 1970; 283: 286–289.
32. McComb JG. Recent research into the nature of cerebrospinal fluid formation and absorption. *J Neurosurg* 1983; 59: 369–383.
33. Eisenberg HM, McLennan JE and Welch K. Ventricular perfusion in cats with kaolin-induced hydrocephalus. *J Neurosurg* 1974; 41: 20–28.
34. Hladky SB and Barrand MA. Mechanisms of fluid movement into, through and out of the brain: evaluation of the evidence. *Fluids Barriers CNS* 2014; 11: 26.
35. Spector R, Robert Snodgrass S and Johanson CE. A balanced view of the cerebrospinal fluid composition and functions: focus on adult humans. *Exp Neurol* 2015; 273: 57–68.
36. Brinker T, Stopa E, Morrison J, et al. A new look at cerebrospinal fluid circulation. *Fluids Barriers CNS* 2014; 11: 10.
37. Cushing HW. The third circulation and its channels. In: *Studies in intracranial physiology & surgery: the third circulation, the hypophysics, the gliomas*. Oxford: H. Milford, Oxford University Press, 1925, pp.1–51.
38. Igarashi H, Tsujita M, Kwee IL, et al. Water influx into cerebrospinal fluid is primarily controlled by aquaporin-4, not by aquaporin-1: 17O JJVCPE MRI study in knockout mice. *Neuroreport* 2014; 25: 39–43.
39. Sonnenberg H, Solomon S and Frazier DT. Sodium and chloride movement into the central canal of cat spinal cord. *Proc Soc Exp Biol Med* 1967; 124: 1316–1320.
40. Trillo-Contreras JL, Ramírez-Lorca R, Hiraldo-González L, et al. Combined effects of aquaporin-4 and hypoxia produce age-related hydrocephalus. Biochim Biophys Acta (BBA) – Mol Basis Dis 2018; 1864: 3515–3526.
41. Bedussi B, van der Wel NN, de Vos J, et al. Paravascular channels, cisterns, and the subarachnoid space in the rat brain: a single compartment with preferential pathways. *J Cereb Blood Flow Metab* 2017; 37: 1374–1385.
42. Rennels ML, Gregory TF, Blaumanis OR, et al. Evidence for a 'paravascular' fluid circulation in the mammalian central nervous system, provided by the rapid distribution of tracer protein throughout the brain from the subarachnoid space. *Brain Res* 1985; 326: 47–63.
43. Lam MA, Hemley SJ, Najafi E, et al. The ultrastructure of spinal cord perivascular spaces: implications for the circulation of cerebrospinal fluid. *Sci Rep* 2017; 7: 12924.
44. Johanson CE, Duncan JA 3rd, Klinge PM, et al. Multiplicity of cerebrospinal fluid functions: new challenges in health and disease. *Cerebrospinal Fluid Res* 2008; 5: 10.
45. Golomb J, Wisoff J, Miller DC, et al. Alzheimer's disease comorbidity in normal pressure hydrocephalus: prevalence and shunt response. *J Neurol Neurosurg Psychiatry* 2000; 68: 778–781.
46. Tulassay T, Khoor A, Bald M, et al. Cerebrospinal fluid concentrations of atrial natriuretic peptide in children. *Acta Paediatr Hung* 1990; 30: 201–207.
47. Silverberg GD, Huhn S, Jaffe RA, et al. Downregulation of cerebrospinal fluid production in patients with chronic hydrocephalus. *J Neurosurg* 2002; 97: 1271–1275.
48. Johanson CE, Szmydynger-Chodobska J, Chodobski A, et al. Altered formation and bulk absorption of cerebrospinal fluid in FGF-2-induced hydrocephalus. *Am J Physiol* 1999; 277: R263–R271.
49. Plog BA, Dashnaw ML, Hitomi E, et al. Biomarkers of traumatic injury are transported from brain to blood via the glymphatic system. *J Neurosci* 2015; 35: 518–526.
50. Lundgaard I, Lu ML, Yang E, et al. Glymphatic clearance controls state-dependent changes in brain lactate concentration. *J Cereb Blood Flow Metab* 2017; 37: 2112–2124.
51. Ma Q, Ineichen BV, Detmar M, et al. Outflow of cerebrospinal fluid is predominantly through lymphatic vessels and is reduced in aged mice. *Nat Commun* 2017; 8: 1434.
52. Tumani H, Huss A and Bachhuber F. The cerebrospinal fluid and barriers – anatomic and physiologic considerations. In: de Vries LS and Glass HC (eds) *Handbook of clinical neurology*. Amsterdam: Elsevier, 2018, pp.21–32.